Simulation of focused wave impact on point absorber wave energy converters - CCP-WSI Blind Test Series 2

Zaibin Lin, Ling Qian, Zhihua Ma, Hao Chen, Derek Causon, and Clive Mingham

Abstract—**This work contributes to the CCP-WSI blind test series 2 by numerically investigates the dynamic response of two simplified point absorber wave energy converters (hemispherical-bottom cylinder and cylindrical moon-pool) under the action of focus waves with varying steepness. The open source toolbox OpenFOAM along with its new overset grid functionality is applied and evaluated for the complex flow problem involving both large free surface deformations and large amplitude motions of floating objects. The quality of numerically generated focused wave groups is first examined and validated against the experimental data. The effects of both wave steepness and the moon-pool on dynamic responses including the mooring force of the simplified wave energy converters (WECs) are then analyzed.**

Keywords—**Floating structures, Focused wave, Overset mesh, Point absorber wave energy converters.**

I. Introduction

CAPTURING energy from ocean waves becomes feasible as a number of prototypes of Wave Energy Converters (WECs) have been proposed and evaluated both experimentally and numerically. As one of the novel WECs, point absorbers are typically designed for the scenarios where wave amplitude is large and wave frequency is close to its structural resonance. Due to the highly nonlinear interactions between waves and point absorber WECs, the motion response of a point absorber WEC under steep ocean waves cannot be fully captured by potential flow based models when wave breaking and significant energy dissipation take place.

In the extreme wave conditions, e.g. represented by focused wave groups, which are formed by a large number of wave components of varying frequencies and amplitudes focusing at a specified location in both space and time, the survivability of WECs needs to be systematically investigated [1]. To this end, substantial progress has been made on numerically investigating the hydrodynamic response and therefore the performance of a moored WEC in water waves [2-4]. Besides, laboratory scaled model tests have also been conducted in order to understand motion response and the snatch load on mooring lines of a WEC in focused waves [5]. It is found that an increased focal wave crest leads to the larger surge and pitch motion response of a hemispherical-bottom WEC. On the other hand, moon-pools have been commonly used in offshore and marine operations, e.g. to launch or recover subsea devices from ships and offshore platforms. Inside the moon-pool piston-like wave resonance often occurs due to the relative vertical motions, resulting in significant amplification of free surface elevation.

This work corresponds to a contribution to the CCP-WSI Blind Test Series 2, which is designed to provide an understanding of the required model fidelity for modelling the behaviour of floating structures. Numerical studies of two types of floating WECs in focused waves are preformed using overset mesh solver in OpenFOAM, which provides a reasonably high fidelity contribution. Two geometries of the simplified WEC are considered, i.e. a hemispherical-bottom cylinder and a hollow cylinder with moon-pool. In the following sections, the mathematical formulae of numerical models are presented, followed by the results and discussions of numerical data, and a brief summary of the work.

II. Mathematical Formulae

A. Equations

In this numerical study, the fluid dynamics is governed by incompressible Navier-Stokes equations which are spatially discretised by the Finite Volume Method as implemented in the open-source toolbox OpenFOAM. A two-phase model, together with the Volume of Fluid method, is applied to describe both the water and air flow

Paper ID/Conference Track: 1463/WHM. This work was supported in part by the EPSRC (UK) under grant No. EP/N008839/1.

Z. Lin, L. Qian, Z. Ma, D. Causon, and C. Mingham are with Centre for Mathematical Modelling and Flow Analysis (CMMFA), Department of Computing, Mathematics and Digital Technology, Manchester Metropolitan University, Manchester, United Kingdom, M15 6BH (e-mail: z.lin@mmu.ac.uk, l.qian@mmu.ac.uk, z.ma@mmu.ac.uk, d.m.causon@mmu.ac.uk, c.mingham@mmu.ac.uk)

H. Chen was at Centre for Mathematical Modelling and Flow Analysis (CMMFA), Department of Computing, Mathematics and Digital Technology, Manchester Metropolitan University, Manchester, United Kingdom. Now he is at Department of Civil and Environmental Engineering, National University of Singapore, 1 Engineering Drive 2, E1A 07-03, Singapore, 117576 (e-mail: ceeche@nus.edu.sg)

as well as their interface. The governing equations for this model are given below:

$$\nabla \cdot \boldsymbol{u} = 0 \tag{1}$$

$$\frac{\partial \rho \boldsymbol{u}}{\partial t} + \nabla \cdot (\rho \boldsymbol{u})\boldsymbol{u}^{\mathrm{T}} - \nabla \cdot (\mu \nabla \boldsymbol{u}) = -\nabla p^{*} - (\boldsymbol{g} \cdot \boldsymbol{x})\nabla \rho \tag{2}$$

$$\frac{\partial \alpha}{\partial t} + \nabla \cdot \boldsymbol{u}\alpha + +\nabla \cdot \left(\boldsymbol{u}_{\boldsymbol{r}}\alpha(1-\alpha)\right) = 0 \tag{3}$$

where $\boldsymbol{u}$ is the velocity field, ρ is fluid density, t is time, μ is dynamic viscosity of fluid; $p^{*} = p - \rho \boldsymbol{g} \cdot \boldsymbol{x}$ is the pressure in excess of static pressure, $\boldsymbol{g}$ is gravitational acceleration, $\boldsymbol{x} = (x, y, z)$ is the Cartesian coordinate system, α is volume fraction field, and $\boldsymbol{u}_{\boldsymbol{r}}$ is compressive velocity field [6], which maintains the sharp water-air interface.

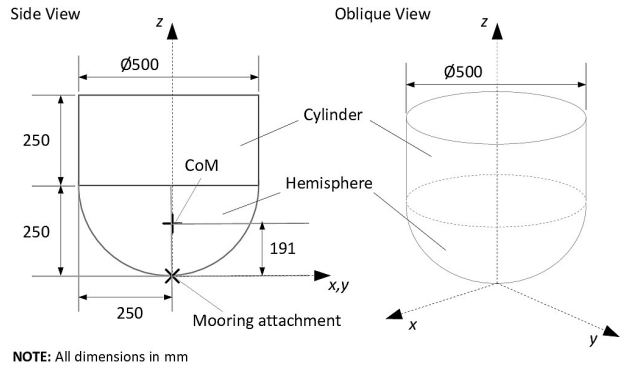

Fig. 1. Sketch of the geometry and dimensions of a hemispherical-bottom cylinder. CoM: Centre of Mass [7].

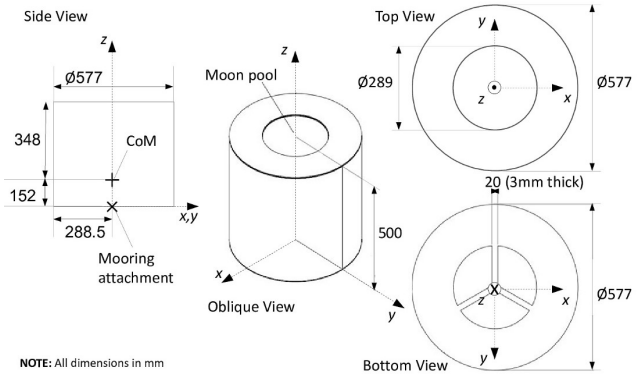

Fig. 2. Sketch of the geometry and dimensions of a cylinder with moon-pool. CoM: Centre of Mass [7].

B. *Overset mesh*

As a recently released functionality in OpenFOAM, overset mesh solver is adopted in this study since it has the capacity of properly capturing large amplitude motions of floating structures under extreme sea states, which may not be adequately resolved by dynamic mesh approach, also implemented in OpenFOAM. Within the overset mesh approach, a composite mesh system is introduced with two layers of mesh: one is the background mesh and the other is the body-fitted mesh. During the simulation, the body-fitted mesh moves with the floating structure as an entity without any mesh deformations, while the background mesh is fixed. These two mesh layers exchange data by interpolation at every time step. Readers are referred to [8, 9] for more details on overset mesh implementations.

C. *Rigid body motion solver*

The six degrees of freedom of WECs are numerically solved by a rigid body motion solver in OpenFOAM (sixDoFRigidBodySolver), whereas a linear spring is used in the mooring system to restrain WECs motions in a numerical wave basin. In this solver, two equations, namely linear and angular momentum conservation equations, are numerically solved to provide the acceleration of WECs. An acceleration relaxation factor of 0.2 is selected in order to stabilize the solution during the simulation. The displacement and velocity of WECs are predicted by integrating the acceleration using the Newmark scheme.

D. *Numerical wave generation*

Here NewWave type focused wave groups are adopted to describe the extreme wave conditions as specified on the blind test series 2 [7]. The wave generation boundary conditions are implemented in IHFOAM [10-14] where the velocity profile and wave amplitude are specified at the inlet boundary on the basis of the second order irregular wave theory [15].

III. RESULTS AND DISCUSSIONS

E. *Experiments*

The experiments of WECs blind tests were conducted in the COAST Laboratory Ocean Basin, Plymouth University, UK. The wave basin is 35m long, 15.5m wide, and 3m deep. In the experiments, two simplified WECs: a hemispherical-bottomed cylinder as illustrated in Fig. 1 and a cylinder with a moon-pool as illustrated in Fig. 2, are tested under the focused wave environments. The corresponding mass properties of two WECs can be found in Table I. The WECs were moored using a linear spring, which is fixed to the wave basin bottom. The spring stiffness of mooring line is 64N/m and the pre-tensions in mooring are 32.07N and 31.55N for the two cases, respectively.

TABLE I
MASS PROPERTIES OF TWO WAVE ENERGY CONVERTERS.

ID	M [kg]	I_{xx} [kgm²]	I_{yy} [kgm²]	I_{zz} [kgm²]	d [m]
1	43.674	1.62	1.62	1.143	0.322
2	61.459	3.56	3.56	3.298	0.330

Note: M is the mass of WECs, I_{xx}, I_{yy}, and I_{zz} are the moment of inertia. d is the draft. ID 1 is the hemispherical-bottom cylinder and ID 2 is the cylindrical moon-pool.

In Table II, the parameters of focused waves generated in the experiment are listed. The crest heights of three focused wave groups are kept the same, while the peak frequencies are different. The target waves were formed by linearly superposing 244 wave fronts, whose frequencies are uniformly distributed between 0.10Hz and 2Hz. In the numerical setup, 13 wave gauges are located based on the laboratory wave gauges layout in Fig. 3, where the buoy was initially located at the focal position of wave group at wave gauge 5. In the final computations, this wave gauge was removed due to the presence of WECs.

TABLE II
TEST CONDITIONS OF THE FOCUSED WAVE GROUPS .

Case	A [m]	T_p [s]	H_s [m]	h [m]	$k_p A$ [-]
1	0.25	2.7949	0.274	3	0.128778
2	0.25	2.5	0.274	3	0.160972
3	0.25	2.2821	0.274	3	0.193167

Note: A is focal crest height, T_p is the wave period for the wave component at peak frequency. H_s is significant wave height, and k_p is wave number for the wave component at the peak frequency.

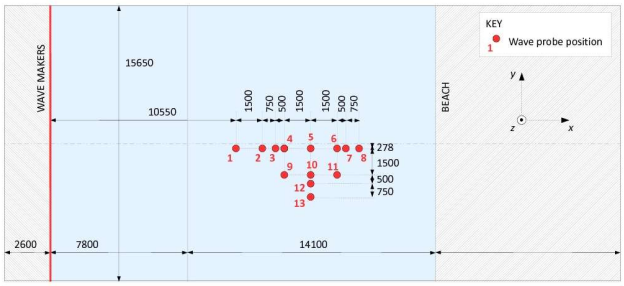

Fig. 3. The layout of wave gauges in the COAST Laboratory Ocean Basin Plymouth University, the UK [7] .

F. *Computational domain and mesh*

The size of the numerical domain is 20m long and 6m wide, corresponding to $1.9\lambda_p$ (λ_p is wave length at peak frequency) and $12D_1$ and $10D_2$ respectively (D_1 is the diameter of the hemispherical-bottom WEC and D_2 is the diameter of the moon-pool WEC). The initial water depth of the numerical domain is 3m, which is the same as that in laboratory. Above the water phase, the height of the air phase is initially set at 1m to allow enough space for the potential WECs motion. The numerical wave groups are focused at 12m away from the wave generation boundary and at 12s in time.

As an overset grid has been applied in this work, two layers of overlapping meshes, namely the background mesh and the minor body-fitted mesh will be generated. For the background mesh, which covers the entire domain and is fixed during the simulation, it is smoothly refined in the vertical direction z, from both the tank bottom and atmospheric boundaries towards the zone with the boundaries of z = -0.3m and z = 0.3m with z = 0m being the initial interface between water and air. Between the two boundaries, the mesh is evenly spaced. In the two horizontal directions, the mesh is stretched smoothly from the domain sides to the focal location. A utility named snappyHexMesh is used here to produce the minor body-fitted mesh, which cuts the background regular hexahedra cells into tetrahedron cells in order to fit an arbitrary solid boundary. In addition, the meshes are refined in the vicinity of two WECs in all three directions. The overall mesh layouts near the WECs are shown in Fig. 4.

Based on the mesh convergence study [16], the mesh with Δx = 0.060m, Δy = 0.061m, and Δz = 0.020m is adopted in the following simulations. The mesh inside the rectangle zone (-1 -0.8 -0.7) (1.5 0.8 0.7) is refined in three directions, which provides sufficient mesh resolution to capture the WECs motions in focused waves.

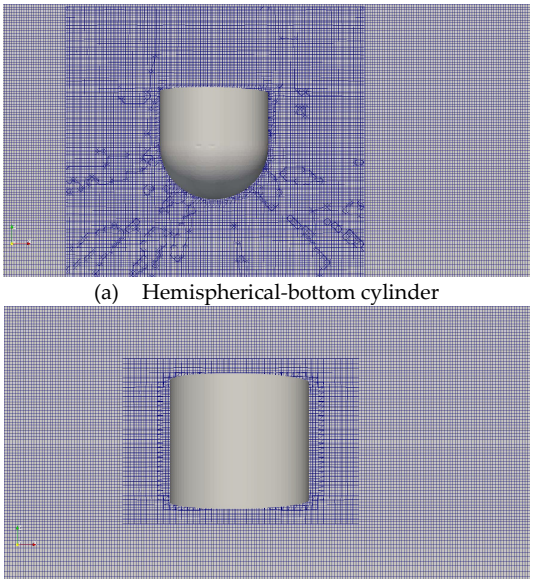

(a) Hemispherical-bottom cylinder

(b) Moon-pool cylinder

Fig. 4. The mesh layouts for overall mesh setups in the vicinity of WECs. (a) Hemispherical-bottom cylinder. (b) Cylindrical moon-pool.

G. *Validation of focused waves generation*

The free surface elevations at Wave Gauges (WGs) 1, 3, 5, and 8 are validated against experimental results in Figs. 5, 6, and 7 for the Case 1, 2, and 3, respectively. In general the generated focused wave groups agree well with measured free surface elevations in the COAST wave basin, especially for the Cases 1 and 2, while slight discrepancy of wave crest at the focal position can be seen in Fig. 7 for Case 3 with the highest wave steepness. This could be attributed to the fact that different wave generation methods have been used in the numerical simulations (fixed boundaries) and experimental studies (wave paddles), despite that a linear superposition of wave fronts is adopted in both approaches. So, the overall quality of the numerically generated focused wave groups is acceptable.

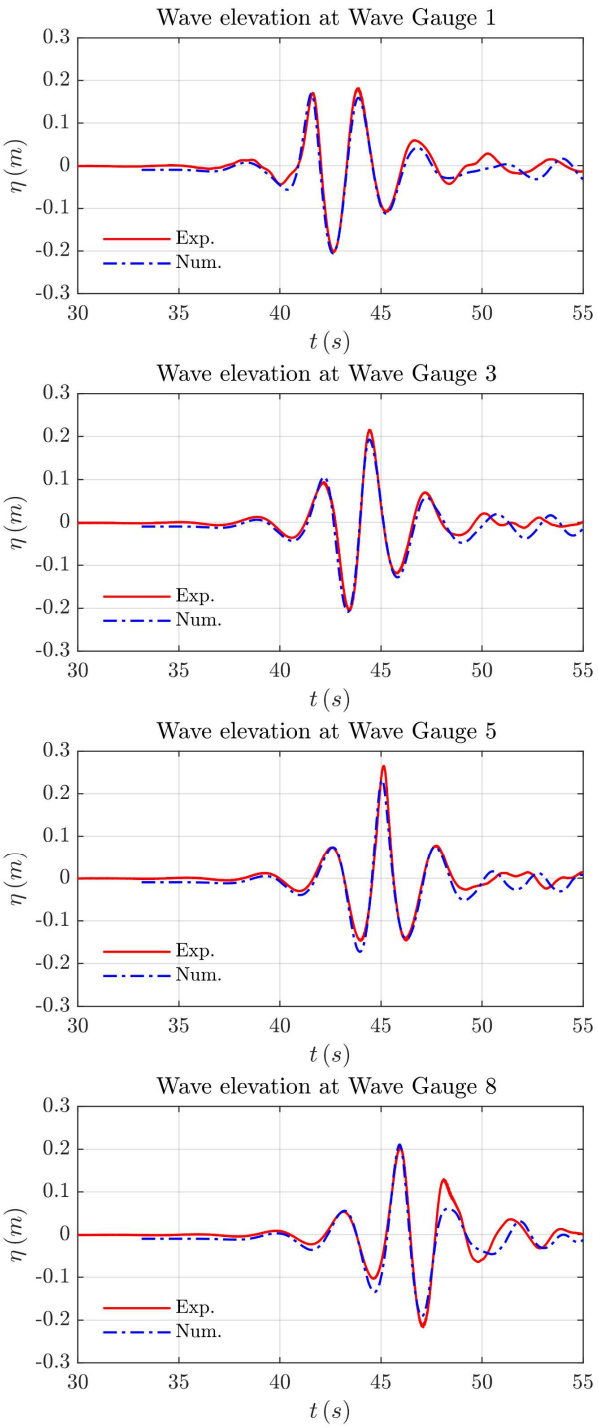

Fig. 5. Comparisons between numerical results of Case 1 against experimental data at four Wave Gauges.

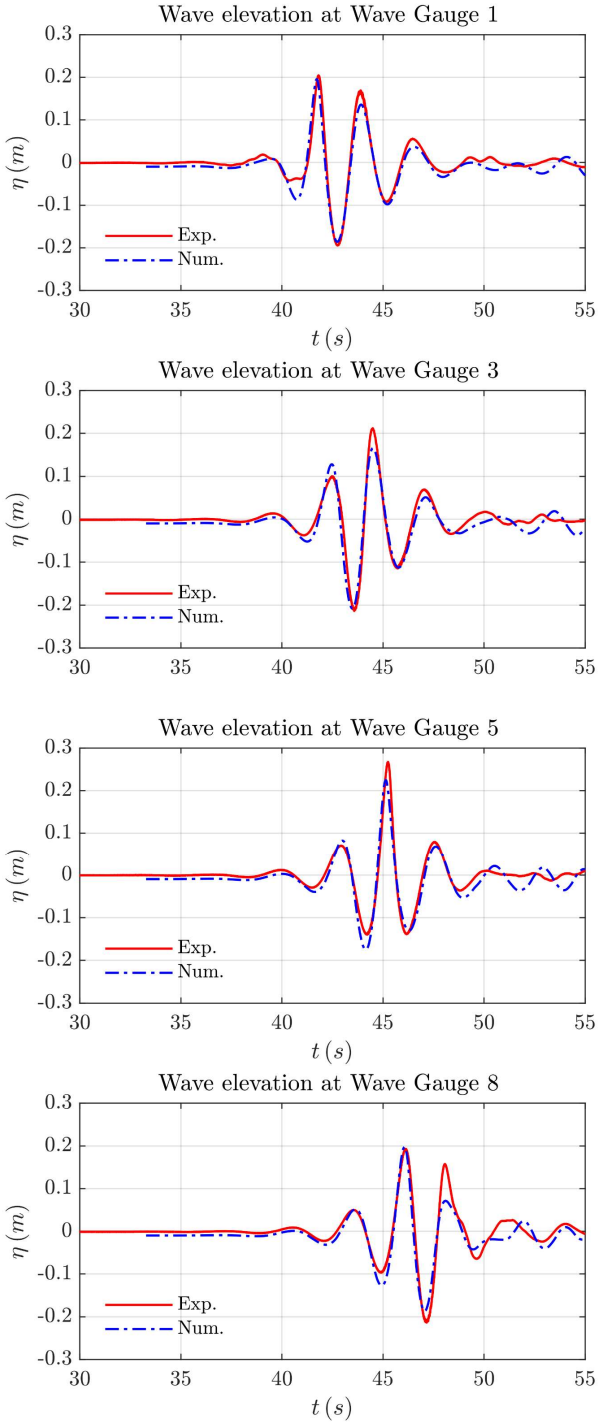

Fig. 6. Comparisons between numerical results of Case 2 against experimental data at four Wave Gauges.

H. Effects of wave steepness on moon-pool cylinder motions

A floating cylinder with moon-pool, subjected in the focused wave with varying peak frequencies, is firstly investigated, in order to understand the effects of wave steepness and WEC geometry on the motion response and mooring force. The focused wave properties are tabulated in Table II. Under these focused wave groups, the motions of the cylindrical moon-pool are presented in Fig. 8, together with the time history of the mooring forces. It is clearly shown that under the condition of the constant focal wave crest, the maximum amplitudes of heave and pitch motions, and mooring force after focal time are similar. However, the surge motion seems to be significantly influenced by the increase of wave steepness. It can be clearly seen from the surge time series that the floating cylinder with moon-pool is drifted away by the incident focused wave, and then takes very long time to return its initial location.

I. Effects of moon-pool on WECs motions and mooring force

As the two WECs shown in Figs. 1-2 have significant differences in geometry, which may result in different/distinct motion responses under same incident waves. In this section, the heave, surge, pitch, and mooring force of the WECs in the same wave conditions (Case 1 in Table II.) are compared in Fig. 9. It can be

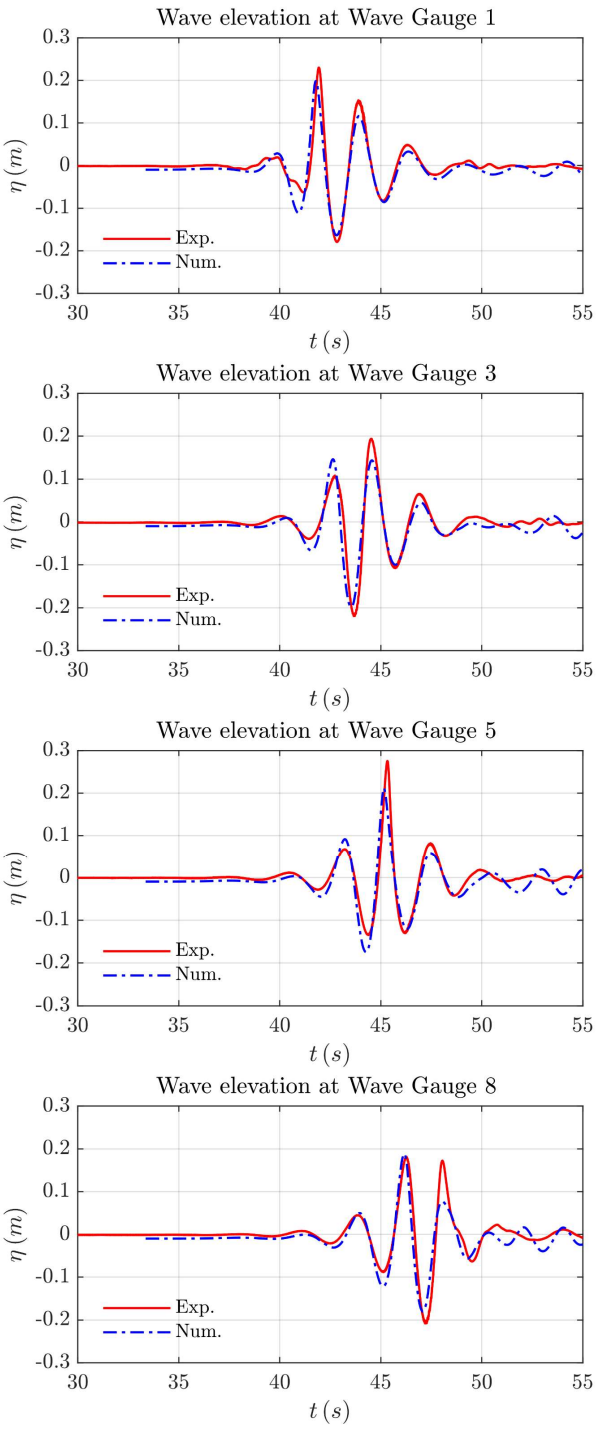

Fig. 7. Comparisons between numerical results of Case 3 against experimental data at four Wave Gauges.

clearly seen that the heave motion and mooring force of both WECs seems to be similar for both peak amplitudes, while significant difference is presented in surge and pitch. For the cylinder with a moon-pool WEC, it requires longer time to return to its initial location (surge = 0m), and the pitch motion decays faster after de-focusing process when compared to that of the hemispherical bottomed WEC. This may be primarily due to the larger moment of inertia of cylindrical moon-pool WEC and viscous effects.

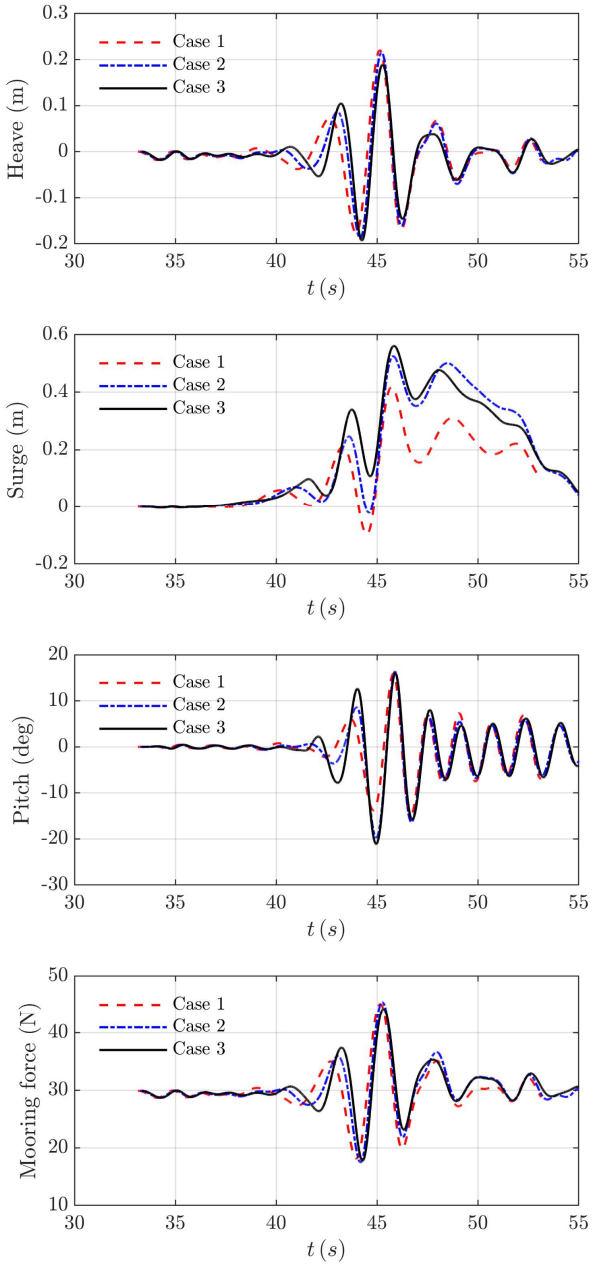

Fig. 8. Heave, surge, pitch, and mooring force of the cases with a cylindrical moon-pool.

IV. CONCLUSIONS

In this paper, the numerical simulations of the two simplified point absorber WECs, namely the hemispherical-bottom cylinder and the floating cylinder with a moon-pool, under focused wave groups are presented, which forms a contribution to the CCP-WSI blind test series 2. Overset mesh in OpenFOAM is adopted to capture the motion response of WECs in the focused wave groups with varying peak frequencies and a constant focused wave crest. The generation of the focused wave was applied to study the motion response of two WECs. It is found that the maximum amplitude and period of heave, pitch, and mooring force for the cylinder with a moon-pool are similar, while the major difference occurs at the surge motion due to the varying peak frequencies and wave steepness. The comparisons of the motions of two WECs with and without a moon-

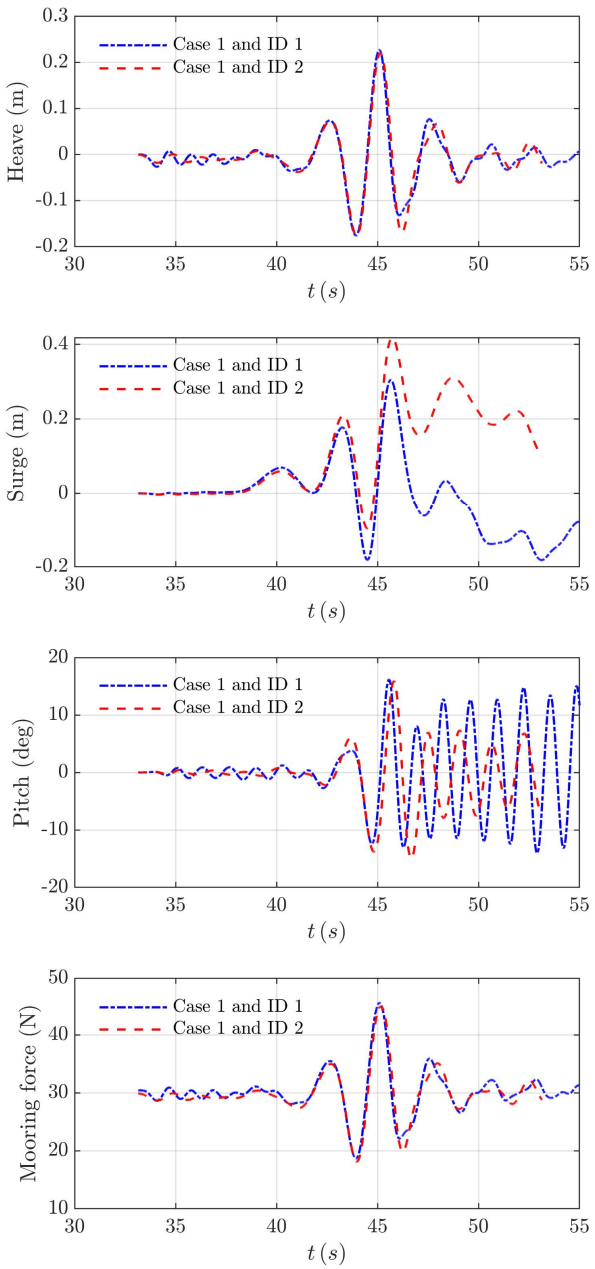

Fig. 9. Comparisons of heave, surge, pitch, and mooring force of the Case 1 between hemispherical-bottom cylinder (ID 1) and cylindrical moon-pool (ID 2).

pool indicate that under the same wave groups, differences in geometry and moment of inertia may lead to distinct surge and pitch motions, although the heave and mooring force tend to be less affected. Subjected to same wave groups, the WEC with moon-pool may be drifted further away (surge motion) from its initial location, while it tends to stabilize faster after the focal time in terms of the pitch motion compared to those of the hemispherical-bottom WEC.

ACKNOWLEDGEMENT

This work was partially funded by the Engineering and Physical Sciences Research Council (EPSRC, UK) Project: A Zonal CFD Approach for Fully Nonlinear Simulations of Two Vessels in Launch and Recovery Operations (EP/N008839/1). The first author would also like to acknowledge the financial support from the Manchester Metropolitan University through sponsoring a Research Associate position.

REFERENCES

[1] Ransley, E., Greaves, D., Raby, A., Simmonds, D., and Hann, M., "Survivability of wave energy converters using CFD," *Renewable Energy*, vol. 109, pp. 235-247, 2017.

[2] Yu, Y.-H., and Li, Y., "Reynolds-Averaged Navier–Stokes simulation of the heave performance of a two-body floating-point absorber wave energy system," *Computers & Fluids*, vol. 73, pp. 104-114, 2013.

[3] Palm, J., Eskilsson, C., Paredes, G. M., and Bergdahl, L., "Coupled mooring analysis for floating wave energy converters using CFD: Formulation and validation," *International Journal of Marine Energy*, vol. 16, pp. 83-99, 2016.

[4] Hu, Z. Z., Causon, D., Mingham, C., and Qian, L., "Numerical simulation of floating bodies in extreme free surface waves," *Natural Hazards Earth System Sciences*, vol. 11(2), pp. 519-527, 2011.

[5] Hann, M., Greaves, D., and Raby, A., "Snatch loading of a single taut moored floating wave energy converter due to focussed wave groups," *Ocean Engineering*, vol. 96, pp. 258-271, 2015.

[6] Berberović, E., van Hinsberg, N. P., Jakirlić, S., Roisman, I. V., and Tropea, C., "Drop impact onto a liquid layer of finite thickness: Dynamics of the cavity evolution," *Physical Review E*, vol. 79(3), pp. 036306, 2009.

[7] "CCP-WSI blind test series 2." [Online]. Available: https://www.ccp-wsi.ac.uk/blind_test_series_2,

[8] Chen, H., Qian, L., Ma, Z., Bai, W., Li, Y., Causon, D., and Mingham, C., "Application of an overset mesh based numerical wave tank for modelling realistic free-surface hydrodynamic problems," *Ocean Engineering*, vol. 176, pp. 97-117, 2019.

[9] Ma, Z., Qian, L., Martinez-Ferrer, P., Causon, D., Mingham, C., and Bai, W., "An overset mesh based multiphase flow solver for water entry problems," *Computers & Fluids*, vol. 172, pp. 689-705, 2018.

[10] Higuera, P., Lara, J. L., and Losada, I. J., "Realistic wave generation and active wave absorption for Navier–Stokes models: Application to OpenFOAM®," *Coastal Engineering*, vol. 71, pp. 102-118, 2013.

[11] Higuera, P., Lara, J. L., and Losada, I. J., "Simulating coastal engineering processes with OpenFOAM®," *Coastal Engineering*, vol. 71, pp. 119-134, 2013.

[12] Higuera, P., Lara, J. L., and Losada, I. J., "Three-dimensional interaction of waves and porous coastal structures using OpenFOAM®. Part I: Formulation and validation," *Coastal Engineering*, vol. 83, pp. 243-258, 2014.

[13] Higuera, P., Lara, J. L., and Losada, I. J., "Three-dimensional interaction of waves and porous coastal structures using OpenFOAM®. Part II: Application," *Coastal Engineering*, vol. 83, pp. 259-270, 2014.

[14] Higuera, P., Losada, I. J., and Lara, J. L., "Three-dimensional numerical wave generation with moving boundaries," *Coastal Engineering*, vol. 101, pp. 35-47, 2015.

[15] Hu, Z. Z., Greaves, D., and Raby, A., "Numerical wave tank study of extreme waves and wave-structure interaction using OpenFoam®," *Ocean Engineering*, vol. 126, pp. 329-342, 2016.

[16] Chen, H., Qian, L., Ma, Z., Bai, W., and Lin, Z., "CFD simulation of wave energy converters in extreme wave conditions," *Proc. The 29th International Ocean and Polar Engineering Conference*, International Society of Offshore and Polar Engineers. Accepted.